Influence of external factors on dielectric permittivity of Rochelle salt: humidity, annealing, stresses, electric field

A.G.Slivka*, V.M.Kedyulich*, R.R.Levitskii**,

A.P.Moina**, M.O.Romanyuk***, A.M. Guivan*

* Uzhgorod National University, 54 Voloshin Street, Uzhgorod, Ukraine

** Institute for Condensed Matter Physics, 1 Svientsitskii Street, Lviv, Ukraine

***Ivan Franko Lviv National University, 8 Kyryla and Mefodiya Street, Lviv, Ukraine

Abstract

The present work contains results of experimental investigation of external factors, such as dessicating/wetting, thermal annealing, uniaxial and hydrostatic pressures on dielectric permittivity of Rochelle salt crystals. The obtained results are compared with available literature data. A conslusion is made that the dispersion of experimental data can be attributed to internal polar point defects in crystals and to influence of storage conditions. The obtained results are analyzed within the phenomenological Landau approach.

1 Introduction

An important information about the transition mechanism in ferroelectric crystals can be given by exploring their behavior under influence of various external factors, such as high pressure or electric field. For hydrogen bonded crystals the external pressures are the only way to continuously vary geometric parameters of bonds, break their equivalence, etc, which permits to investigate role of hydrogen bonds and their parameters and symmetry in mechanisms of the phase transition and dielectric response of the crystals. Many of ferroelectrics are piezoelectric in the paraelectric phase; application of shear stresses and the conjugate electric fields provides a possibility to explore the role of piezoelectric interactions in the phase transitions and in formation of the physical characteristics of the crystals.

The above mentioned possibilities were fully used for investigation of the KH_2PO_4 family crystals. Theoretical description of pressure and field effects in these crystals are usually performed within the proton ordering model (see e.g. [1, 2, 3, 4, 5, 6] and references therein) and a quantitative agreement with experiment is obtained. It was shown, in particular, that pressures of different symmetries can produce qualitatively different changes in the phase transition: lower its temperature down (hydrostatic), raise it up and smear out the transition (as shear stress σ_6), induce a new phase of monoclinic symmetry (as $\sigma_1 - \sigma_2$).

In contrast to the KH_2PO_4 family crystals, the data for external factors influence on Rochelle salt crystals are less extensive. In literature, only a few papers are available on hydrostatic pressure [7, 8, 9] and electric field [11, 10, 12] effects on the dielectric permittivity of the crystals. Uniaxial stresses effects on the phase transitions in Rochelle salt were explored in in [13] from the measurements of thermoelastic effect. Theoretically influence of the shear stress σ_4 was studied in [14] within the modified Mitsui model.

Usually, peculiarities of the physical characteristics of ferroelectric crystals in the vicinity of the phase transitions (especially of the second order ones) are affected by crystal defects and internal bias electric fields and mechanical stresses, which act as the external ones. The role of such factors, as crystal defectness and the processes in the sample prehistory, that may affect the physical properties of the crystals via relaxation of the defects: thermal annealing, previous influence of electromagnetic fields and mechanical stresses, must be explored. High pressure and electric field studies allow to explore the intrinsic field and pressure dependences of the crystal properties, reveal the internal bias fields and stresses, and study the residual effects of the internal defects.

For Rochelle salt, whose chemical instability (loss of crystallization water at slightly elevated temperatures) and water absorbency are well known, other factors such as air humidity, storage conditions, etc are important and should be monitored during measurements. For instance, a significant dispersion of experimental data for the dielectric permittivity of Rochelle salt (see the systematization in [15]), exceeding the measurement error, takes place. Apparently, the dispersion is due to the different internal states of the samples, not controlled during measurements.

In the present work the results of experimental studies of the mentioned above external factors (pressure, electric field, humidity, thermal annealing) influence on dielectric permittivity of Rochelle salt crystals in the vicinity of the structural phase transitions are reported.

2   Experimental setup

Dielectric permittivity of the crystals ε_{11} was determined by measuring the samples capacity with the help of an a.c. bridge at fixed frequency of 1 kHz. Measurement error was $0.2 \div 0.4\%$.

Samples were prepared in a form of parallellepipeds, with faces perpendicular to crystallographic axes of an orthorhombic (paraelectric) unit cell. Silver paste and copper wires, $0.08 \div 0.12$ mm diameter, were used as electric contacts. After partial drying of the paste, the contacts were covered by an alcohol solution of a glue with addition of silver paste. This method provided a necessary mechanical stability of the contacts and allowed a free deformation of the crystals.

A uniaxial pressure was created by a spring dynamometer and transmitted to samples via a punch with floating heads, thus securing a uniform pressure even at possibly non-parallel faces of the sample. The pressure was fixed with an accuracy of $\pm 5\%$. The samples were placed in a thermostate, allowing smooth adjustment of temperature. Temperature was measured by a copper-constantan thermocouple with an accuracy ± 0.1 . Samples with the thermocouple were covered with silicone oil, in order to enhance heat transmission and prevent direct contact with air.

3   Model approach

Theoretical description of the physical properties of Rochelle salt is usually performed within a two-sublattice Ising model with asymmetry double well potential (Mitsui model). Below we present the expression for the dielectric permittivity of Rochelle salt obtained within the modified Mitsui model with taking into account the piezoelectric coupling [15] with the Hamiltonian

$$\hat{H} = \frac{N}{2} v c_{44}^{E0} \varepsilon_4^2 - N v e_{14}^0 \varepsilon_4 E_1 - \frac{N}{2} v \chi_{11}^0 E_1^2 - \frac{1}{2} \sum_{qq'} \sum_{ff'=1}^{2} R_{qq'}(ff') \frac{\sigma_{qf}}{2} \frac{\sigma_{q'f'}}{2}$$

$$- \Delta \sum_q \left(\frac{\sigma_{q1}}{2} - \frac{\sigma_{q2}}{2} \right) - (\mu_1 E_1 - 2\psi_4 \varepsilon_4) \sum_q \sum_{f=1}^{2} \frac{\sigma_{qf}}{2}.$$

Three first terms in (3.1) correspond to a 'seed" energy of the crystal lattice which forms the asymmetric double-well potential for the pseudospins. $R_{qq'}(11) = R_{qq'}(22) = J_{qq'}$ and $R_{qq'}(12) = R_{qq'}(21) = K_{qq'}$ are constants of interaction between pseudospins belonging to the same and to different sublattices, respectively. The parameter Δ describes the asymmetry of the double well potential; μ_1 is the effective dipole moment. The last term is the internal field created by the piezoelectric coupling with the shear strain ε_4.

Within a mean field approximation the static dielectric permittivity of a free crystal is obtained in the form [15]

$$\chi_{11}^{\sigma} = \chi_{11}^{\sigma 0} + \frac{\beta (\mu_1')^2}{2v} F_2(0), \tag{3.1}$$

where ξ, σ are the parameters of ferroelectric and antiferroelectric ordering. The following notations are used

$$F_2(0) = \frac{\varphi_3}{\varphi_2 - \Lambda \varphi_3},$$

$$\varphi_2 = 1 - \frac{\beta J}{2} \lambda_1 - \beta^2 \frac{K^2 - J^2}{16} (\lambda_1^2 - \lambda_2^2), \quad \varphi_3 = \lambda_1 + \beta \frac{K-J}{4} (\lambda_1^2 - \lambda_2^2), \quad \Lambda = \frac{2\beta \psi_4^2}{v c_{44}^{E0}},$$

$$\lambda_1 = 1 - \xi^2 - \sigma^2, \qquad \lambda_2 = 2\xi\sigma,$$

$$d_{14}^0 = \frac{e_{14}^0}{c_{44}^{E0}}, \quad \chi_{11}^{\sigma 0} = \chi_{11}^{\varepsilon 0} + e_{14}^0 d_{14}^0, \quad \mu_1' = \mu_1 - 2\psi_4 d_{14}^0.$$

Values of the model parameters providing the best fit to the permittivity are given in Table 1.

Table 1: Model parameters for Rochelle salt [15].

J/k_B	K/k_B	Δ/k_B	ψ_4/k_B	c_{44}^{E0}	d_{14}^0	$\chi_{11}^{\sigma 0}$
		K		dyn/cm^2	esu/dyn	
797.36	1468.83	737.33	-760	$12.8 \cdot 10^{10}$	$1.9 \cdot 10^{-8}$	0.363

$v = 0.5219[1 + 0.00013(T - 190)] \cdot 10^{-21}$ cm^3

4 Influence of sample prehistory on dielectric permittivity of Rochelle salt

4.1 Humidity

In [17] it was found that crystals of Rochelle salt at 25° and relative humidity below 40% lose the crystallization water, whereas at relative humidity above 85% they absorb water from air. Experimentally, significant changes of the piezoelectric properties of Rochelle salt were observed, when samples are kept in air with high concentration of ethanol vapor [16].

Experimental data for the susceptibility of Rochelle salt of different sources (see fig. 1) show an essential dispersion, even in the paraelectric phases, which cannot be accounted for by the changes in the measurements regimes. Of interest was thus to explore the temperature dependences of Rochelle salt crystals with different water content, in order to verify whether this dispersion can be attributed, at least partially, to it.
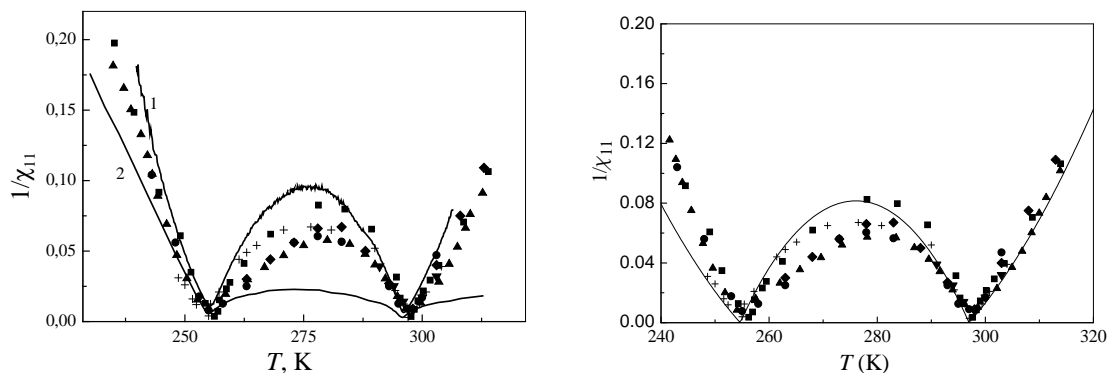
Figure 1: Temperature dependences of inverse susceptibility of Rochelle salt. Left: solid lines – experimental data, this work, obtained for 1 – dessicated sample; 2 – wet sample. Right: solid line – theoretical curve, calculated with (3.1). ■ – [18]; ▲ – [19]; ◆ – [20]; ● – [21]; ▼ – [22]; + – [23].

The obtained results are presented in fig. 1 (left). Apart from the literature data, we show here the temperature dependences of the inverse dielectric susceptibility χ_{11}^{-1} (solid curves 1 and 2), obtained in this work for the same sample with different water content. The curve 1 is obtained for a sample, kept for a long time (2–3 days) at room temperature in a closed volume, filled with a dessicator (silicagel). The curve 2 corresponds to the same sample, kept for 10 hours in air with relative humidity ∼90%. As one can see, keeping the sample in a wet air decreases the dielectric susceptibility in the entire studied temperature range. The changes are particularly prominent in the middle of the ferroelectric phase $T \sim 275$ K and in the high-temperature paraelectric phase.

Comparison of the obtained results with literature data shows that the dispersion in the values of the susceptibility indeed can be caused by a different water content in the samples used in different experiments. It should be also noted that for a wet sample (curve 2, fig. 1), a linear temperature dependence of inverse susceptibility $\chi^{-1}(T)$ with the Curie-Weiss constant $C_W = 1.95 \cdot 10^3$ K. For a dessicated sample, the dependence $\chi^{-1}(T)$ is non-linear in both paraelectric phases.

Comparison of literature experimental data with the theoretical ones, obtained in [15] from the formula (3.1), is given in fig. 1 (right). Theoretical absolute values of the permittivity are adjusted by the choice of the value of the effective dipole moment μ_1. In [15] μ_1 was chosen such as the best agreement with the data of [22] as well as of the dynamic microwave permittivity is obtained. On this, we, however, failed to get an adequate agreement with experiment for susceptibility in the low-temperature paraelectric phase [15].

4.2   Influence of thermal annealing

Fit. 2 illustrates the temperature dependences of dielectric permittivity of Rochelle salt near the upper Curie point for samples annealed at 308 K. On increasing the annealing time, the value of the dielectric permittivity at the transition point increases, and the maximum temperature decreases. Such changes are apparently caused by internal electrical bias fields, which magnitude is decreased with increasing annealing time.
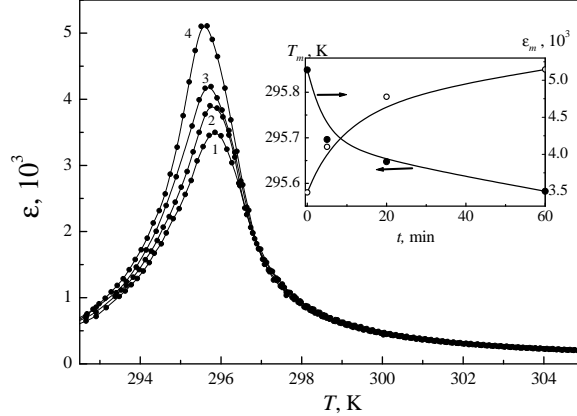
Figure 2: Temperature dependences of the dielectric permittivity of Rochelle salt near the upper transition point at different times of annealing in the paraelectric phase at 308 K (min): $1 - 0$, $2 - 5$, $3 - 20$, $4 - 60$. Inset: dependences of the maximal value of permittivity and maximum temperature on annealing time.

The internal bias fields are created by polar defects [24], which at long-term keeping samples in the ferroelectric phase participate in screening of spontaneous polarization and reflect the corresponding domain structure. Action of the internal bias field is analogous to the action of external field, that is, the temperature of the upper maximum of permittivity is increased, and the maximum magnitude is decreased. In the next section we shall estimate the magnitudes of the internal bias fields in the non-annealed and annealed samples.

5   Influence of external electric field

In fig. 3 we show the measured temperature dependences of dielectric permittivity ε_{11} of Rochelle salt crystals near the upper and lower transition points at different values of external d.c. electric field $E = E_1$ applied along the ferroelectric axis (conjugate to polarization). The insets contain the field dependences of the dielectric permittivity maxima ε_m and their temperatures $\Delta T_m = T_m(E) - T_m(0)$. The data are obtained by cooling samples for the upper maximum and by heating for the lower one (from the corresponding paraelectric phase towards the ferroelectric phase). As expected, the external field, conjugate to polarization, decreases the ε_m and shifts the maxima temperatures ΔT_m in a non-linear way. For the upper maximum $\Delta T_{m2} > 0$, whereas for the lower one $\Delta T_{m1} < 0$.
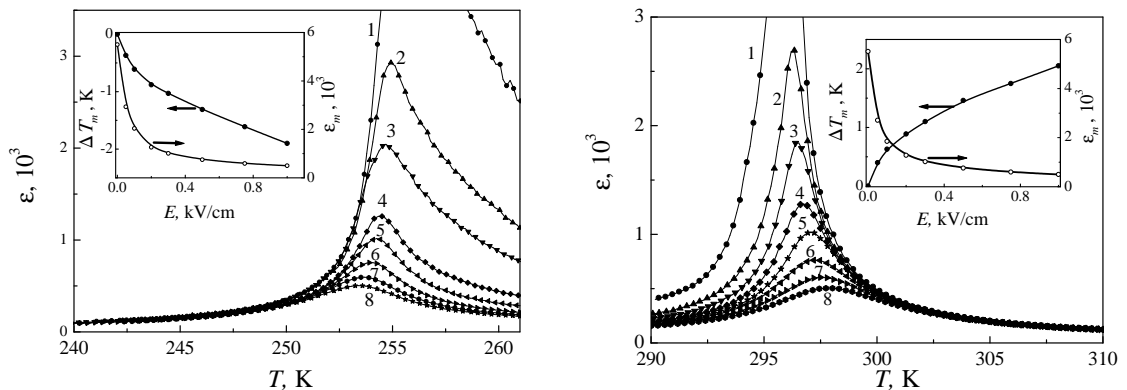
Figure 3: Temperature dependences of the dielectric permittivity of Rochelle salt crystals near upper and lower transition points at different values of external electric field E_1 (kV/cm): $1 - 0$, $2 - 0.05$, $3 - 0.1$, $4 - 0.2$, $5 - 0.3$, $6 - 0.5$, $7 - 0.75$, $8 - 1$. Lines are guide to the eyes.

These results are compared in fig. 4 with literature data obtained from the field dependences of permittivity [25] and elastic compliance s_{44}^E [10]. The obtained in this work field dependences of the permittivity maxima magnitudes ε_m^{-1} are the same for the two maxima (see fig. 4) and well accord with the data of [25]. However, a perceptible disagreement is observed for the shift of the permittivity maxima temperatures. Our data yield very close changes of $|\Delta T_m|$ with field for the two maxima. On the contrast, the obtained in [25] field dependence of the upper maximum temperature is much stronger that of the lower one.

For Rochelle salt the phenomenological Landau expansion of the thermodynamic potential can be presented as

$$\Phi(P_1) = \Phi_0 + \frac{\alpha}{2}P_1^2 + \frac{\beta}{4}P_1^4, \tag{5.2}$$

where P_1 is the crystal polarization, α, β are the expansion coefficients. The electric field E_1 is applied along the axis of spontaneous polarization [100].
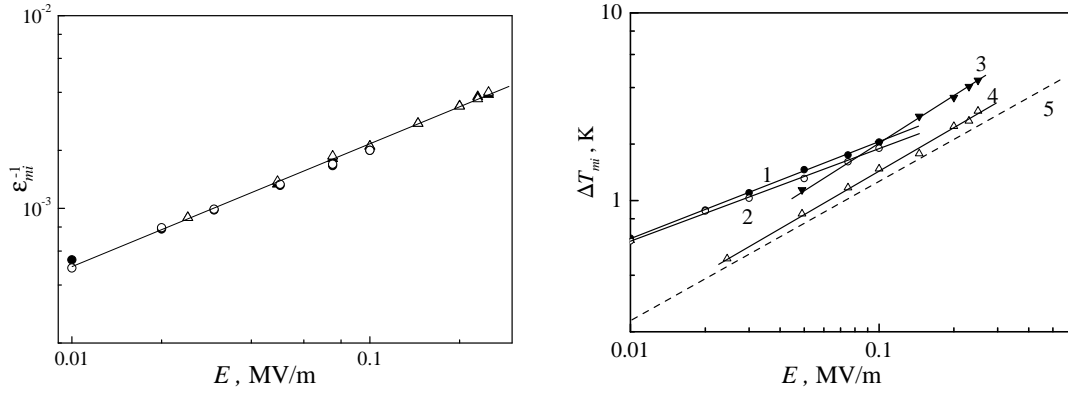
Figure 4: Field dependences of the permittivity maxima magnitudes (left) and temperature shifts (right). Upper maximum: curve 1 and $\bullet$ – this work, curve 3 and $\blacktriangledown$ – [16], curve 5 – [10]. Lower maximum – curve 2 and $\circ$ – this work, curve 4 and $\triangle$ – [16].
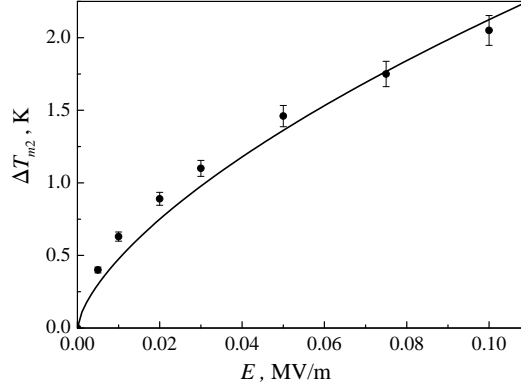
Figure 5: Field dependence of the upper permittivity maximum temperature shift. Line is calculated with (5.4). Symbols are experimental data of this work.

For Rochelle salt there are two possible ways to model the temperature dependence of the coefficient α.

1) The expansion (5.2) is performed near each of the two transitions separately, assuming a linear temperature dependence $\alpha = \alpha_{T1}(T_{C1} - T)$ for the lower transition and $\alpha = \alpha_{T2}(T - T_{C2})$ for the upper one. Then the field dependences of $\varepsilon_m(E_1)$ and $\Delta T_m(E_1)$ can be presented as

$$\varepsilon_m^{-1} = \frac{3}{2}\frac{(4\beta)^{1/3}}{4}\varepsilon_0 E_1^{2/3} = k_1 E_1^{2/3}. \tag{5.3}$$

$$|\Delta T_{mi}| = \frac{3}{4}\frac{(4\beta)^{1/3}}{\alpha_{Ti}}E_1^{2/3} = k_2 E_1^{2/3}, \quad i = 1, 2 \tag{5.4}$$

2) Within the second approach, the coefficent α is chosen in the form

$$\alpha = \alpha_1 + \alpha_2(T - T_0)^2, \tag{5.5}$$

where $T_0 = \frac{T_{C1}+T_{C2}}{2}$, and $T_{C1,2} = T_0 \mp \sqrt{-\frac{\alpha_1}{\alpha_2}}$. Such a choice is validated by the fact that the phase transitions in Rochelle salt are closed to a double critical point [26, 10], realized at partial substitution of potassium atoms with ammonia NH_4 [27, 11]. In [26, 10] the temperature dependences of several physical characteristics of Rochelle salt were successfully described within the Landau approach with (5.5).

In this case, the field dependences of $\Delta T_m(E_1)$ are

$$\Delta T_{m1,2} = \pm A \mp \sqrt{\frac{3}{4} \frac{(4\beta)^{1/3}}{\alpha_{T2}} E_1^{2/3} + A^2},\tag{5.6}$$

where $A^2 = -\alpha_1/\alpha_2$. The field dependence of $\varepsilon_m(E_1)$ in this case is the same as in the first approach and described by (5.3).

The experimental dependences of $\varepsilon_m^{-1}(E_1)$ of this work are well described by equation (5.3) with $k_1 = 10.2 \cdot 10^{-7} (m/V)^{2/3}$ and $\beta = 11.34 \cdot 10^{13}$ $V \cdot m^5/C^3$. Fitting to the experimental data for $\Delta T_m(E_1)$ with eq. (5.4), shown in Fig. slivka6c, yields the values of k_2 and α_{T1}, α_{T2} for the upper and lower maxima:

$$\text{for} \quad T_{C1}: \quad k_2 = 9.9 \cdot 10^{-4} \ (m/V)^{2/3} \quad \text{and} \ \alpha_{T1} = 5.82 \cdot 10^7 \ V \cdot m \cdot (K \cdot C)^{-1};$$

$$\text{for} \quad T_{C2}: \quad k_2 = 10.5 \cdot 10^{-4} \ (m/V)^{2/3} \ \text{and} \ \alpha_{T2} = 5.49 \cdot 10^7 V \cdot m \cdot (K \cdot C)^{-1}.$$

Agreement with experiment for $\Delta T_m(E_1)$, obtained with formulas (5.6) is not any better than with (5.4). We found that
$\alpha_1 = -5.82 \cdot 10^8$ $V \cdot m \cdot C^{-1}$, $\alpha_2 = 1.32 \cdot 10^6$ $V \cdot m \cdot C^{-1 \cdot -2}$.

Advantages of this approach are visible only at description of the physical characteristics of Rochelle salt in a sufficiently wide temperature range in the paraelectric phases, where the non-linear temperature dependence of the inverse permittivity should be essential. However, for description of the field dependences of $\Delta T_m(E_1)$ the non-linearity of the coefficient α within a few Kelvins near the transition points does not play any significant role.

Description of the field dependences of the dielectric permittivity of Rochelle salt within a modified Mitsui model with piezoeffect will be given in another publication.

Using the above results, we can estimate the magnitude of internal bias fields, existing in crystals without annealing and after 60 min of annealing. In the former and latter cases, the values of the permittivity at the upper transition point are about 3500 and 5100 (see fig. 2). Therefore, using (5.3) and the found values of k_2, we get that at the upper Curie point $E_{bias} = 0.055$ kV/cm for a non-annealed sample and $E_{bias} = 0.027$ kV/cm for the sample annealed for 60 min.

6   External pressures

6.1   Uniaxial stresses

The temperature dependences of dielectric permittivity ε_{11} of Rochelle salt were measured at 1 kHz and different values of mechanical stresses applied along the main crystallographic directions of unit cell: $[100] - \sigma_1$, $[010] - \sigma_2$, $[001] - \sigma_3$ and along $[011] - \tilde{\sigma}_4$. In the reference system with axes along the main crystallographic directions, the stress $\tilde{\sigma}_4$ can be presented as

$$\tilde{\sigma}_4 = \sigma_4 + \frac{1}{2}(\sigma_2 + \sigma_3),\tag{6.1}$$

where σ_4 is the shear strain, which for the Rochelle salt symmetry is the external field conjugate to the order parameter and acts similarly to the electric field E_1.

Figs. 6-9 contain the obtained temperature dependences of dielectric permittivites at different values of the uniaxial pressures and the corresponding stress dependences of the permittivity maxima temperatures. The data, as in the case of electric field study, were obtained at cooling for the upper maximum and at heating for the lower maximum (on going from the corresponding paraelectric phase towards the ferroelectric phase).

Similarly to the electric field E_1, all explored uniaxial stresses decrease the maximal values of the dielectric permittivity and change their temperatures T_{m1} and T_{m2}. Action of the stresses σ_1 and $\tilde{\sigma}_4$ on T_{m1} and T_{m2} is non-linear and similar to the action of the electric field E_1: $dT_{m1}/d\sigma_i < 0$; $dT_{m2}/d\sigma_i > 0$ ($i = 1$ and $\tilde{4}$). It should be noted that the change of the upper maximum temperature with the stress $\tilde{\sigma}_4$ is much larger than of the lower maximum. Let us remind that the obtained in this work changes of the maxima temperatures with the electric field E_1 are almost the same for the two maxima (see figs. 4, 5).
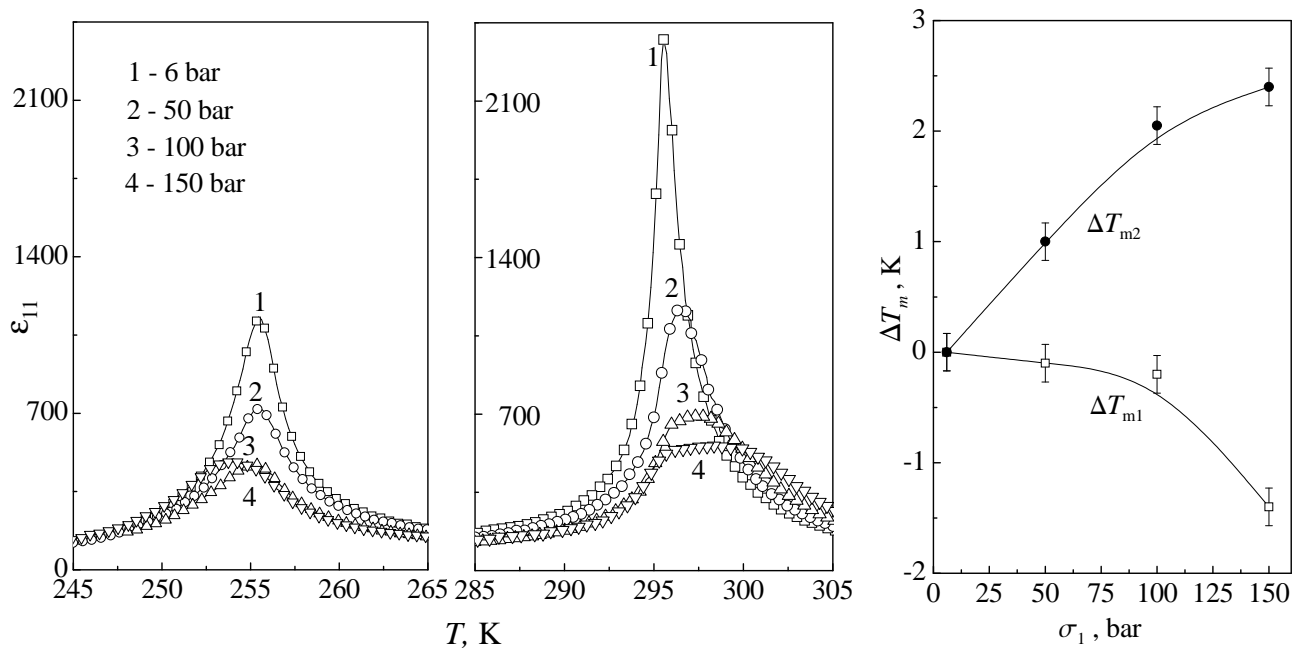
Figure 6: Temperature dependences of the dielectric permittivities of Rochelle salt at different values of mechanical stress σ_1 and the stress dependences of the permittivity maxima temperatures.
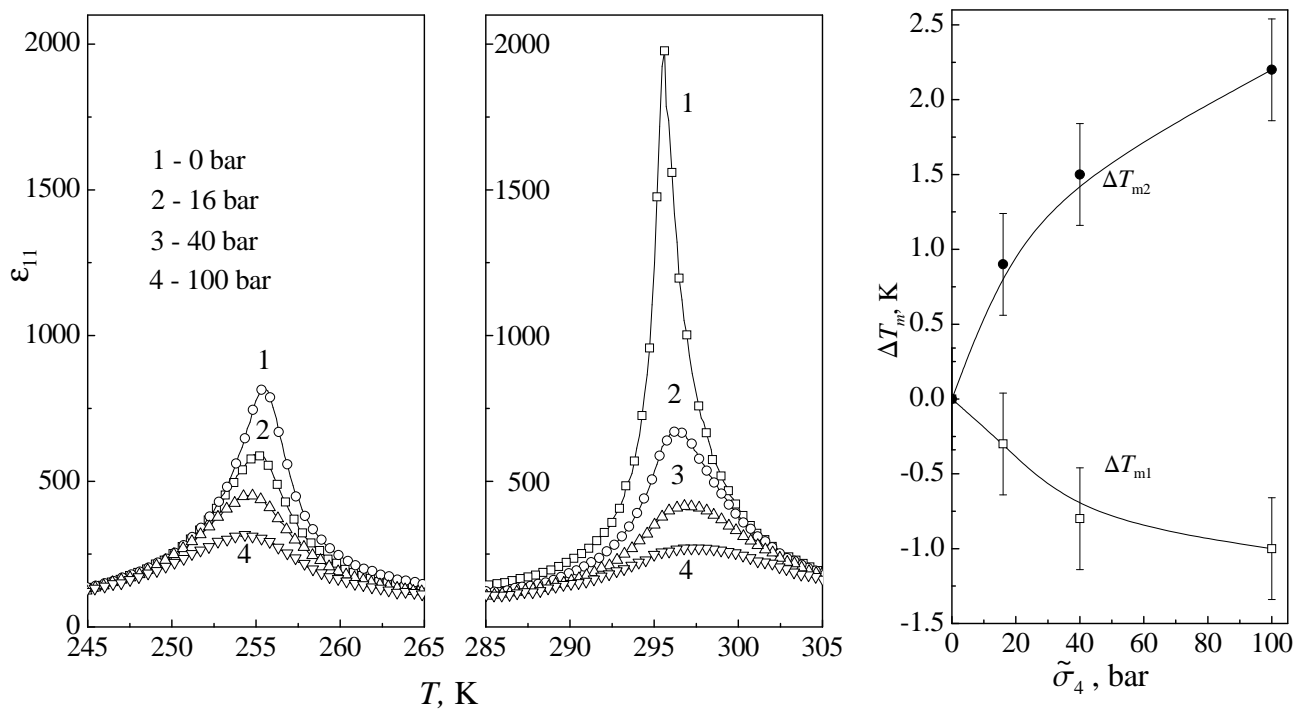
Figure 7: Same for the stress $\tilde{\sigma}_4$.
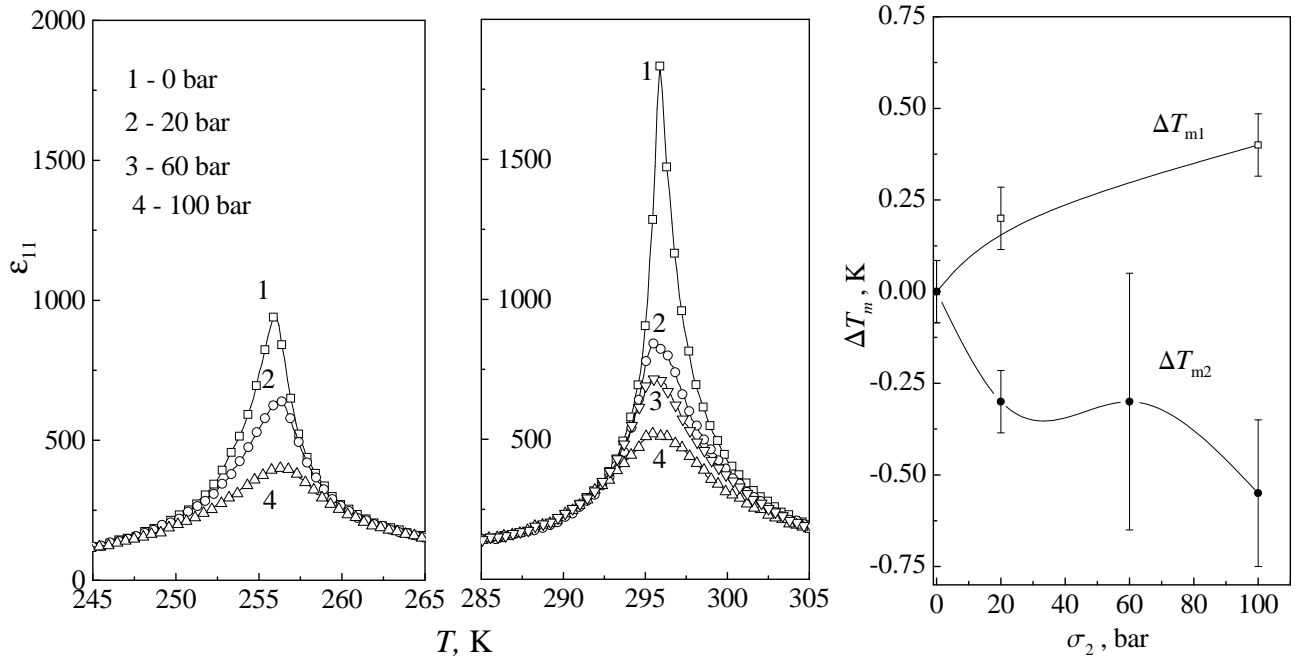
Figure 8: Same for the stress σ_2.
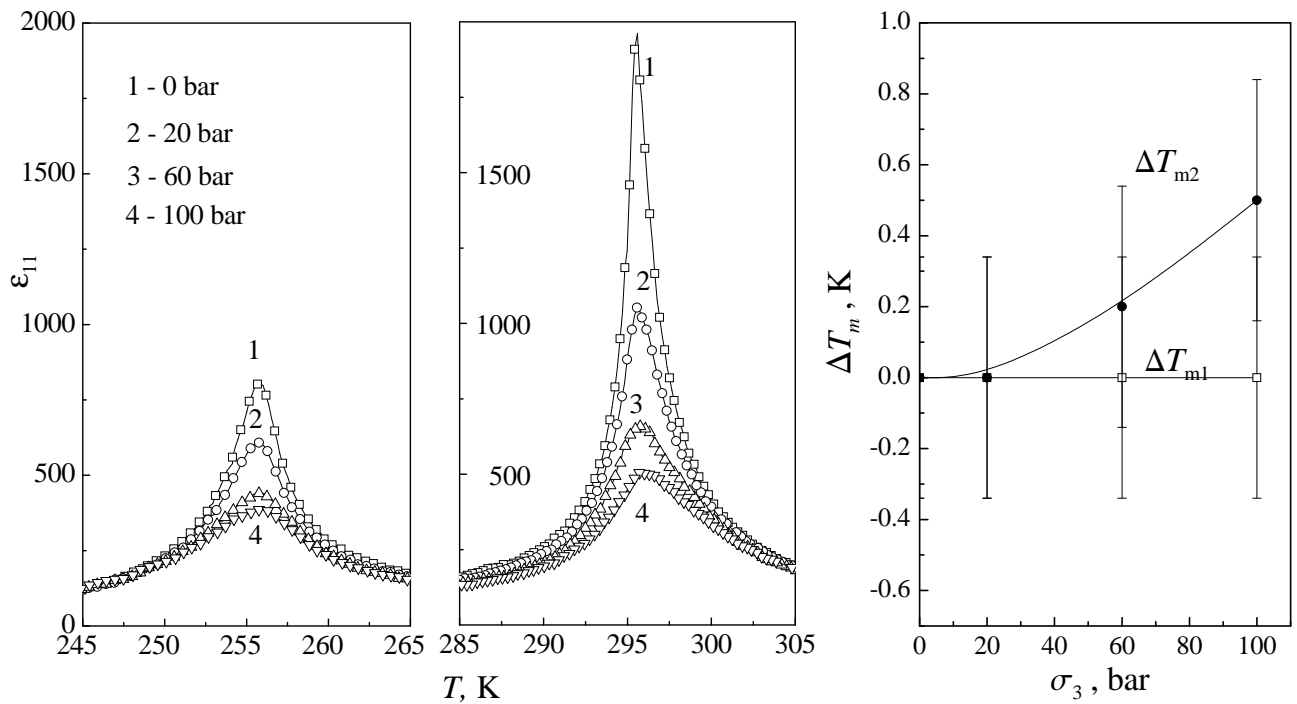
Figure 9: Same for the stress σ_3.

The experimental data for the shifts of the transition temperature with the uniaxial stresses (per 100 bar) are systemized in Table 3. For comparison, we present here the corresponding literature data obtained in [13] on the basis of thermoelastic effect. Overall, the obtained in this work data qualitatively agree with the literature data, except for the case of stress σ_3. However, the quantitative agreement is rather poor, our data for $|\Delta T_{Ci}|$ being a few times smaller.

6.2 Hydrostatic pressure

Fig. 10 contains the temperature dependences of the dielectric permittivity of Rochelle salt at different hydrostatic pressures. In contrast to electric field or uniaxial stresses, the hydrostatic pressure increases both transition temperatures (see the inset with the p, T-diagram). The pressure coefficients of the transition temperatures are $dT_{C1}/dp = 3.54$ K/kbar and $dT_{C2}/dp = 10.92$ K/kbar, in a perfect agreement with the data of [7, 8]. On increasing the hydrostatic pressure, the value of ε_m at the lower transition point T_{C1} monotonously decreases and remains unchanged at T_{C2}.
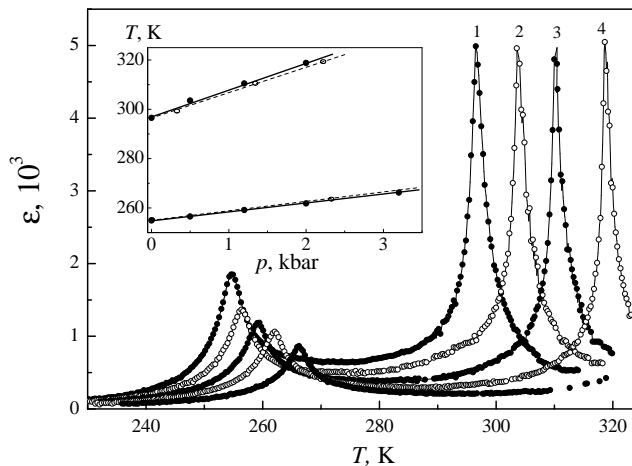
Figure 10: Temperature dependence of the dielectric permittivity of Rochelle salt at different values of hydrostatic pressure p, MPa: 1 – 0; 2 – 50; 3 – 120; 4 – 200; 5 – 320. Inset: the p, T phase diagram. Dashed lines and ∘ – data of [7].

6.3 Phenomenological description of pressure effects

For phenomenological description of external pressure influence on the phase transitions in Rochelle salt, let us modify the expansion (5.2) in the following way

$$\Phi(P_1, \sigma_i) = \Phi_0 + \frac{\alpha}{2}P_1^2 + \frac{\beta}{4}P_1^4 + \sum_{i=1}^{3} q_{i1}\sigma_i P_1^2 + g_{14}P_1\sigma_4 - \frac{1}{2}\sum_{ij=1}^{4} s_{ij}^P \sigma_i \sigma_j \tag{6.2}$$

(for the sake of simplicity we changed here the signs the stresses σ_i, in comparison with the standard notations, so that the uniaxial compression stresses are positive, and for the hydrostatic pressure we have $p = \sigma_1 = \sigma_2 = \sigma_3$. In standard notations $-p = \sigma_1 = \sigma_2 = \sigma_3$ and values of the compression stress are negative.) The quantities q_{i1} have a meaning of electrostriction coefficients, s_{ij}^P are the elastic compliances at constant polarization. Let us note that s_{ij}^P for $i = 1, 2, 3$ and s_{44}^P are practically temperature independent, whereas $s_{i4}^P \sim P_1$, that is, they are different from zero only in the ferroelectric phase or in presence of electric field (possibly internal bias field E_{bias} due to polar defects) or stress σ_4.

From (6.2) the equations for polarization and lattice strains follow

$$E_1 = g_{14}\sigma_4 + (\alpha + 2\sum_{i=1}^{3} q_{i1}\sigma_i)P_1 + \beta P_1^3 - \sum_{i=1}^{3} \frac{s_{i4}^P}{P_1}\sigma_i \sigma_4 \tag{6.3}$$

$$u_i = \frac{\partial \Phi}{\partial \sigma_i} = -\sum_{j=1}^{4} s_{ij}^P \sigma_j + q_{i1}P_1^2, \quad i = 1, 2, 3 \tag{6.4}$$

$$u_4 = g_{14}P_1 - \sum_{j=1}^{4} s_{ij}^P \sigma_j. \tag{6.5}$$

Assuming a linear dependence of the coefficient $\alpha = \alpha_{T1}(T_{C1} - T)$ for the lower transition and $\alpha = \alpha_{T2}(T - T_{C2})$ for the upper one, we get for the transition temperatures shift and the inverse values of the permittivity of a free crystal (at constant stress)

$$\Delta T_{C1,2} = \pm \frac{2}{\alpha_{T1,2}} \sum_{i=1}^{3} q_{i1}\sigma_i \mp k_1(E_{bias} - g_{14}\sigma_4)^{2/3} \tag{6.6}$$

$$\varepsilon_{m1,2}^{-1} = k_2\left(E_{bias} - g_{14}\sigma_4 + \sum_{i=1}^{3} \frac{s_{i4}^P}{P_1}\sigma_i\sigma_4\right)^{2/3}. \tag{6.7}$$

Experimental data for g_{14} are rather dispersive (see the systematization in [15]). We used here the theoretical data for g_{14} of [15], agreeing overall with experiment. The electrostriction coefficients have been determined in [28]. We use adjusted here their values, in order to get a good fit to the hydrostatic pressure dependences of transition temperatures. The used values of q_{i1}, g_{14} at lower and upper transition points are given in table 2.

Table 2: The used data for q_{i1} (in m^4/C^2) and g_{14} (in m^2/C).

	q_{11}	q_{21}	q_{31}	g_{14}
T_{C1}	-7.5	4	4.5	0.174
T_{C2}	-10	4.3	2.5	0.195

We consider first the case of a perfect crystal ($E_{bias} = 0$). The calculated shifts of the transition temperatures (permittivity maxima temperatures) with uniaxial and hydrostatic pressures are presented in table 3. As one can see, a very good agreement is obtained with the hydrostatic pressure data, as well as the data of [13] for the uniaxial stresses. Agreement with the calculation data for $\tilde{\sigma}_4$ is completely unsatisfactory. Here we used an assumption that, according to (6.1), $\tilde{\sigma}_4 = 100$ bar corresponds to a sum of $\sigma_4 = 50$ bar, $\sigma_2 = 50$ bar, $\sigma_3 = 50$ bar. Our data for the uniaxial stresses are also in a poor agreement with the phenomenology and with the literature data; however, the data calculations and of [13] agree fairly well.

Table 3: Shifts of the transition temperatures with uniaxial stresses (per 100 bar) and with hydrostatic pressure (per 1 kbar).

	σ_1			σ_2			σ_3			$\tilde{\sigma}_4$		hydrostatic	
	exp.	[13]	calc.	exp.	[13]	calc.	exp.	[13]	calc.	exp.	calc.	exp.	calc.
T_{C1}	**-1.2**	-2.9	-2.73	**0.4**	1.5	1.46	**0**	1.7	1.63	**-1.0**	-8.8	**3.43**	3.64
T_{C2}	**2.0**	3.5	3.44	**-0.6**	-1.6	-1.48	**0.5**	-0.8	-0.86	**2.2**	9.1	**10.92**	10.99

It seems likely that the disagreement between the experimental data of this work and of [13] should be attributed to the influence of sample defects. We recalculated the shifts of the maxima temperature with uniaxial pressure with taking into account also the role of internal bias field, determining them from (6.7). A much better agreement was obtained for the stresses σ_2 and σ_3: $|\Delta T_{Ci}|$ decrease by several times with increasing $E_{bias} = 0$. However, for the stress σ_1, the presence of the bias field has further enhanced the theoretical values $|\Delta T_{Ci}|$, only worsening an agreement with the experimental data of this work. At the moment, we have no complete explanation of the disagreement between our experimental data and the data of [13] and of the calculations, especially in a view of the fact that for the hydrostatic pressure a complete coincidence with the literature data and with phenomenology is obtained.

The reasons for the strong decrease of permittivity maxima magnitude with diagonal stresses σ_i, $i = 1, 2, 3$ is not quite clear either. As follows from (6.7), such a decrease can be accounted for by the increase of the internal bias field E_{bias} or of the coefficient $k_2 \sim \beta^{1/3}$. Such an increase of k_2 can be obtained if we take into account the terms of the fourth order of the $\sum_{i=1}^{3} q_{i1}^{(4)}\sigma_i P_1^4$ type in the expansion (6.2). Effectively it would lead to renormalization of the coefficient $\beta \to \beta + 4\sum_{i=1}^{3} q_{i1}^{(4)}\sigma_i$.

7 Conclusions

- Strong dependence of the dielectric permittivity of Rochelle salt on humidity of the storage air is shown. We believe that the dispersion of experimental data of different literature sources can be caused by uncontrolled water content during and previously to the measurements.

- Dependence of the permittivity value at the transition points on duration of thermal annealing in high-temperature paraelectric phase indicate the existence of internal electric bias fields in the crystals due to point polar defects.

- Influence of external electric field, uniaxial stresses, and hydrostatic pressure on the dielectric permittivity is studied. The results are compared with available literature data. Analysis of the obtained results is performed within the phenomenological Landau approach. Possible reasons for discrepancies in the data are discussed.

Acknowledgement

References

[1] Stasyuk I.V., Levitskii I.V., Moina A.P., Phys. Rev. B., 1999, **59**, 8530.

[2] Stasyuk I.V. Levitskii R.R., Zachek I.R., Moina A.P., Phys. Rev B., 2000, **62**, 6198.

[3] Stasyuk I.V., Levitskii R.R., Zachek I.R., Duda A.S., Condens. Matter Phys., 2001, **4**, 553.

[4] Levitskii R.R., Slivka A.G., Moina A.P. et al, Journ. Phys. Studies., 2002, **6**, No. 2, 197.

[5] Stasyuk I.V., Levitskii R.R. *et al*, Journ. Phys. Studies, 1999, **3**, 502.

[6] Stasyuk I.V., Levitskii R.R., Moina A.P., Velychko O.V., Ferroelectrics, 2003, **2**88, 133.

[7] Bancroft D., Phys.Rev., 1938, **53**, 587.

[8] Samara G.A., J. Chem. Solids, 1965, **26**, 121.

[9] Samara G.A., J. Chem. Solids, 1969, **29**, 870.

[10] Serdobolskaya O.Yu., Sol. Stat. Phys., 1996 **38**, 1529.

[11] Gesi K., Ozawa K., J. Phys. Soc. Japan, 1992, **48**, 2003.

[12] Ismailzade I.H., Samedov O.A., Alekberov A.I., phys. stat. sol.(a), 1986, **94**, K17.

[13] Imai K., Journ. Phys. Soc. Japan, 1975, **39**, 868.

[14] Levitskii R. R., Zachek I. R., Moina A.P., Verkholyak T.M., J. Phys. Studies, 2003, **7**, 106.

[15] Levitskii R.R., Zachek I.R., Verkholyak T.M., Moina A.P., Phys.Rev.B., 2003, **67**, 174112.

[16] Valasek J., Phys. Rev., 1922, **20**, 639.

[17] W.P. Mason, *Piezoelectric Crystals and Their Application to Ultrasonics* (Van Nostrand, New York, 1950).

[18] Hablützel J., Helv. Phys. Acta,1939, **12**, 489.

[19] Taylor W., Lockwood D.J., Labbe H.J., J. Phys. C.: Solid State Phys., 1984, **17**, 3685.

[20] Mueller H., Phys. Rev., 1935, **47**, 175.

[21] Mason W.P., Phys. Rev., 1939, **55**, 775.

[22] Petrov V.M., Kristallografiya (Sov. Phys.— Crystallogr.), 1962, **7**, 403.

[23] Yurin V.A., Bull. Ac. Sci USSR, Phys. Ser. , 1965, **29** 2001.

[24] Lines M., Glass A. Principles and application of ferroelectrics and related materials, Clarendon Press, Oxford, 1977.

[25] Akishige Y., Kamishina Y., J. Phys. Soc. Japan, 1992, **61**, 4589.

[26] Kryukova E.B., Sobyanin A.A.,Bull. Ac. Sci USSR, Phys. Ser. , 1987, **51** 2090.

[27] Makita Y., Takagi Y., J. Phys. Soc. Japan, 1958, **13**, 367.

[28] Schmidt G., Z. Phys., 1961, **1**64, 579.